ACS OMEGA

http://pubs.acs.org/journal/acsodf

Article

Coassembly Generates Peptide Hydrogel with Wound Dressing Material Properties

Chaitanya Kumar Thota, Allison A. Berger, Laura Elomaa, Chaunxiong Nie, Christoph Böttcher, and Beate Koksch*

Cite This: *ACS Omega* 2020, 5, 8557−8563

Read Online

ACCESS | Metrics & More | Article Recommendations | Supporting Information

ABSTRACT: Multicomponent self-assembly of peptides is a powerful strategy to fabricate novel functional materials with synergetic properties that can be used for several nanobiotechnological applications. In the present study, we used a coassembly strategy to generate an injectable ultrashort bioactive peptide hydrogel formed by mixing a dipeptide hydrogelator with a macrophage attracting short chemotactic peptide ligand. Coassembly does not impede hydrogelation as shown by cryo-transmission electron microscopy (cryo-TEM), scanning electron microscopy, and rheology. Biocompatibility was shown by cytotoxicity assays and confocal microscopy. The hydrogels release the entrapped skin antibiotic ciprofloxacin, among others, in a slow and continuous manner. Such bioinspired advanced functional materials can find applications as wound dressing materials to treat chronic wound conditions like diabetic foot ulcer.

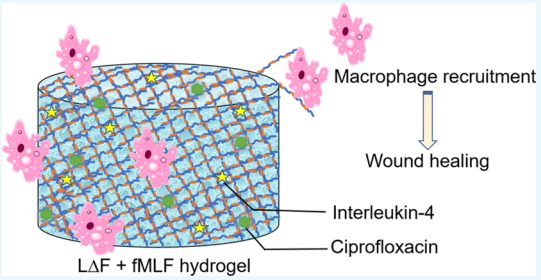

INTRODUCTION

Molecular self-assembly plays a pivotal role in bottom-up approaches to fabricating nanoscale materials with biotechnological applications.[1] In particular, biocompatible peptide based architectures like vesicles, nanosheets, nanospheres, nanotubes, and nanofibers generated by this means can serve as tools for nanomedicine.[2−8] For example, self-assembly in peptides can lead to the formation of self-supporting three-dimensional hydrogels that are composed of nanofiber networks with high water content and high mechanical strength and that are biodegradable and biocompatible with organisms.[1,4,7−10] Thus, they can act as reservoirs for the slow and continuous release of entrapped bioactive molecules and can also mimic the extracellular matrix, which enables their use as drug delivery agents and as scaffolds for tissue engineering. In addition to all these above features, peptide-based gels are relatively easy and inexpensive to synthesize, characterize, and decorate, which makes them more advantageous compared to several other natural and synthetic hydrogels.[10]

Numerous hydrogelators based on fluorenylmethoxycarbonyl (Fmoc)-modified oligopeptides, canonical and noncanonical single aromatic amino acids, DOPA, fluorinated Fmoc-derivatives, and naphthyl-modified alanine have been reported.[11−15] In these cases, stacking interactions between Fmoc groups typically drive self-assembly. An alternative to the Fmoc group is the nonproteinogenic amino acid α,β-dehydrophenylalanine (ΔPhe), which is known to trigger the formation of hydrogels in the context of the ultrashort sequence **LΔF** (Figure 1A).[9] Such hydrogels can be conjugated with different bioactive ligands that induce growth and differentiation of various cell types. Functionalization can be achieved by either pre- or post-self-assembly covalent conjugation strategies.[16−19] The main disadvantage of the former is that the hydrogelating property of the short sequence can be compromised by even small covalent modifications; the main disadvantage of the latter is that subsequent to hydrogelation the groups to be modified may be inaccessible, resulting in low modification efficiency and batch-to-batch variation. For these reasons, supramolecular peptide coassembly has emerged as a promising approach.[20−23] This noncovalent approach is presently being used to generate different novel structures with applications as light harvesting soft materials, in catalysis, in enhancing the mechanical strength of materials, and in tissue engineering.[22]

In the present study, we report a coassembly strategy for generating an injectable ultra-short bioactive peptide hydrogel that could be developed as a wound dressing material. The components are the dipeptide hydrogelator **LΔF** and **fMLF** (Figure 1A), the shortest known chemotactic factor that attracts macrophages.[24−26] Macrophage recruitment plays a key role in wound healing, wherein the M2 phenotype secretes a wide variety of growth factors (GFs) that in turn trigger a cascade of events that attract several other cells, like fibroblasts,

Received: December 19, 2019
Accepted: March 5, 2020
Published: April 7, 2020

https://dx.doi.org/10.1021/acsomega.9b04371
ACS Omega 2020, 5, 8557−8563

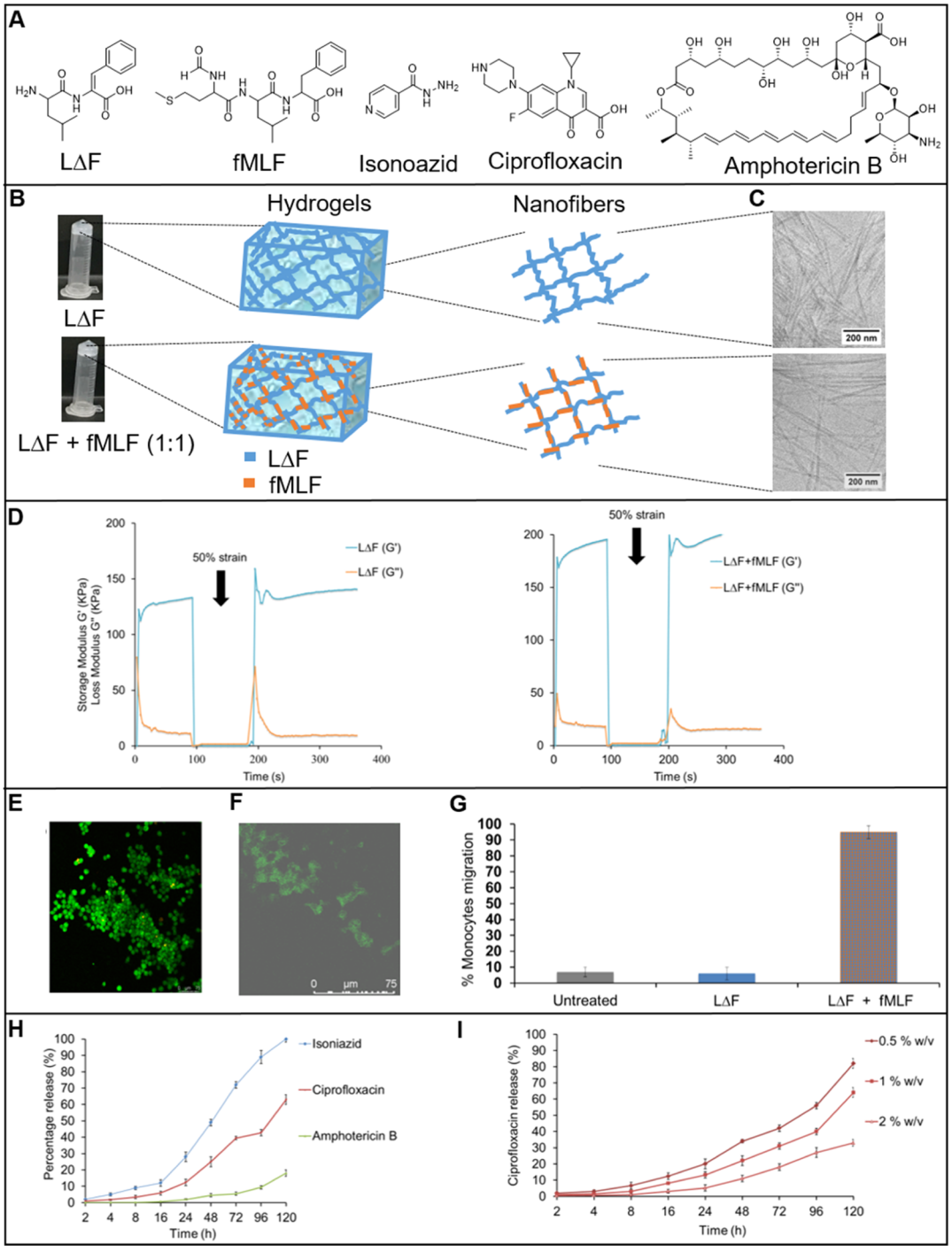

Figure 1. (A) Line structures of **LΔF**, **fMLF** isoniazid, ciprofloxacin, and amphotericin B. (B) Inversion test showing self-supporting hydrogels of **LΔF** alone (upper) and **LΔF** + **fMLF** (1:1) (lower) and cartoons of hydrogels and the nanofibers comprising them in each case. (C) Cryo-transmission electron microscopy (cryo-TEM) analysis of **LΔF** (upper) and **LΔF** + **fMLF** (1:1) (lower) hydrogels. (D) Time-dependent step-strain rheological tests of **LΔF** and **LΔF** + **fMLF** (1:0.5) showing injectability and self-healing properties. Confocal microscopy images showing viability of (E) U937 macrophages and (F) fibroblasts in 1% w/v **LΔF** + **fMLF** (1:0.5). (G) Monocyte/macrophage migration assay with untreated cells, **LΔF** alone, and 1% w/v **LΔF** + **fMLF** (1:0.25). (H) Release profiles for isoniazid, ciprofloxacin, and amphotericin B from 1% w/v **LΔF** + **fMLF** (1:0.25) hydrogel over a period of 5 days. (I) Release profile for ciprofloxacin from 0.5, 1, or 2% w/v **LΔF** + **fMLF** (1:0.25) hydrogel over a period of 5 days.

that aid in wound closure.[27−29] A strategy such as this, which ensures that endogenous GFs are spontaneously and continuously supplied to the wound site, circumvents the need to exogenously provide these in the form of recombinant proteins that suffer from limitations due to their high cost of production, low efficacy and safety, and rapid degradation in vivo.[30−32]

RESULTS AND DISCUSSION

Coassembly and Hydrogel Characterization. **LΔF** was prepared according to a previously reported solution phase

https://dx.doi.org/10.1021/acsomega.9b04371
ACS Omega 2020, 5, 8557−8563

synthetic route (Supporting Information).[9] **fMLF** was synthesized on a solid support according to the Fmoc strategy (Supporting Information). **LΔF** was coassembled with increasing amounts of **fMLF** peptide ligand in the **LΔF**/**fMLF** ratios 1:0.25, 1:0.5, and 1:1 (Supporting Information), and the hydrogel properties of the mixtures were analyzed at 1% w/v in 0.8 M sodium acetate buffer, unless otherwise indicated. A standard tube inversion test was carried out to determine the formation of self-supporting hydrogels (Figure 1B), a property that **fMLF** alone does not have (data not shown). All samples assembled to form self-supporting hydrogels, indicating that **fMLF** does not perturb hydrogelation of **LΔF**.

To determine the elemental composition of the coassembled nanofibers, energy-dispersive X-ray spectroscopy (EDX) analysis of the hydrogels was carried out. Figure S3 shows the EDX spectra of the nanofibers, in which the signals for carbon (C), nitrogen (N), oxygen (O), sodium (Na), and sulfur (S) are labeled accordingly. As expected, the spectrum of **LΔF** displays no signal for sulfur, whereas the coassembled nanofibers show sulfur contents that increase with **LΔF**/**fMLF** ratio: 0.99% (1:0.25), 2.46% (1:0.5), and 3.08% (1:1). This provides evidence that the nanofibers resulting from the peptide mixtures are composed of both **LΔF** and **fMLF** peptides.

Cryo-TEM analysis was performed to quantify the effect of coassembly on the dimensions of the nanofibers that comprise the hydrogel. Figure 1B shows cryo-TEM images of the extreme cases **LΔF** and **LΔF**/**fMLF** (1:1), for which nanofibers of diameter of 13 ± 2 and 16 ± 2 nm, respectively, are observed (Figure S4). This suggests that the thickness of the nanofibers that comprise the **LΔF** hydrogel increases in the presence of **fMLF**, a trend that is also observed in the intermediate samples 1:0.25 (14 ± 1 nm) and 1:0.5 (16 ± 2 nm) (Figures S4 and S5). The ultrastructure of the hydrogels was determined by scanning electron microscopy (SEM). Figure S6 shows dense networks of nanofiber bundles in all cases. From a qualitative perspective, the thickness of the bundles appears to increase with the concentration of the **fMLF** peptide. The apparent increase in nanofiber diameter could be attributed to intermolecular interactions, most likely $\pi-\pi$ stacking interactions between the phenyl (**fMLF**) and dehydrophenyl groups (**LΔF**) of the two components.

To understand the effect of coassembly on peptide secondary structure, circular dichroism (CD) studies were performed and the values were normalized based on extinction coefficient, path length, peptide concentration, and the number of residues (Figure S7). **LΔF** was reported to form β-like as well as extended structures and shows a characteristic strong minimum at 275 nm.[9] This is attributed to an excitation split in the electronic transition state of the ΔPhe chromophore that originates with a rigid mutual disposition of two or more ΔPhe residues. CD studies indicated a slight decrease in intensity of the minima at 275 nm with the increase in the **fMLF** content in the mixtures; however, there is no indication of any significant secondary structural change.

Taken together, the EDX, cryo-TEM, SEM, and CD data indicate that **LΔF** and **fMLF** indeed coassemble within hydrogel structures. The properties of these hydrogels were further characterized in the context of a potential wound dressing material.

Mechanical Strength/Injectability. Injectability of wound dressing materials can provide defect margin adaptation at the wound site.[33−35] The rheology-based shear-thin recovery of peptide hydrogels and the underlying mechanism was first reported by Schneider and co-workers.[36,37] In order to determine the thixotropic behavior of the coassembled gels reported here, the samples were subjected to time-dependent step-strain rheological tests (Figure 1D). Storage modulus (G') values were measured for samples at 1% w/v. The G' value of **LΔF** alone is 132 kPa and that of **LΔF**/**fMLF** (1:1) is 189 kPa. These values indicate that these coassembled hydrogels belong to the class of soft hydrogels, materials which have been shown, when multivalently displaying bioactive ligands, to have potential applications in targeted drug delivery, tissue engineering, and wound healing.[20,27,38−41] The frequency sweep rheology experiments (1−100 rad/s) carried out indicate high stabilities for both samples, as the G' and G'' (loss modulus) values were found to be independent of frequency.

In these rheology tests, first a low strain (0.1%) was used, followed by the application of a high strain (50%) and then a reversion of strain back to 0.1%. The high strain of 50% here represents the kind of force typically experienced by the hydrogels during uptake into a syringe. Both **LΔF** and **LΔF**/**fMLF** (1:1) possess a solid gel-like structure ($G' > G''$) with stable and higher G' and G'' values during the initial 0.1% low strain. With the application of a high strain of 50%, a transition from solid gel into liquid-like material is indicated by the rapid decline in G' and G'' values, with $G' < G''$. Upon reverting to 0.1% low strain, the gels appear to regain their original strength, with $G' > G''$. These data indicate that coassembly does not alter the injectability of **LΔF** and that the ligand mixed hydrogels also have the ability to withstand stress and to self-heal.

Biocompatibility. Biocompatibility is essential for the successful application of wound dressing materials. Thus, the viabilities of HEK293T, macrophages, and fibroblasts upon exposure to **LΔF** and the coassemblies at 0.5, 1.0, and 1.5% w/v were determined. Figure S8 shows the CCK8-based cell viability assay conducted on the hydrogels seeded with cells after 48 h of plating. None of the hydrogel formulations shows any toxicity to the tested cell lines. This would indicate the potential of these ligand coassembled hydrogels for use as scaffolds for wound therapy. Furthermore, the hydrogels were tested for their ability to act as three-dimensional scaffolds for the growth of macrophages and fibroblasts. Figures 1E,F show images obtained by confocal microscopy studies indicating viability of both cell lines in **LΔF**/**fMLF** gels. The cell culture was continuously supplemented with IL4 to maintain macrophages in the M2 phenotype. The proliferation of fibroblasts in 1% w/v **LΔF** + **fMLF** (1:0.25) was analyzed indirectly by PrestoBlue assay, which indicated a progressive increase in cellular metabolism of these cultures from day 0 to day 14 (Figure S9).

Macrophage Recruitment. Wound dressing materials that recruit macrophages to the wound site are beneficial as they can enable a continuous supply of endogenous GFs. To find the ability of the **LΔF**/**fMLF** hydrogel to attract U937 monocyte/macrophage, a chemotactic migration assay was performed, which shows that coassembly does not affect the chemoattractant property of **fMLF** (Figure 1G).

Drug Entrapment and Release. Infections at the wound site can hamper the healing process in normal wounds, and, in the case of chronic wound conditions like diabetic foot ulcer (DFU), it usually leads to amputation. Such complications

https://dx.doi.org/10.1021/acsomega.9b04371
ACS Omega 2020, 5, 8557−8563

currently necessitate the need for the coadministration of antibiotics at the wound site to prevent infection. The drawbacks to conventional drug delivery methods are that repeated administration of the drug is required and that this is characterized by burst release. Such burst release profiles are undesirable because they can be pharmacologically dangerous, causing unnecessary nonspecific cytotoxicity, not to mention that this type of administration route is economically inefficient due to the need for a large excess of the drug.

As an alternative, hydrogel matrices composed of a network of nanofibers can be used as a reservoir to entrap and release small-molecule drugs, macromolecular drugs, and even engineered cells in a slow and continuous manner controlled by diffusion. Furthermore, the hydrogel matrix can reduce degradation of the entrapped drug. The applicability of peptide gels for slow and continues release of entrapped drugs and GFs is widely reported.[42−46] In order to determine the drug release profiles of **LΔF** and coassembled 1% w/v **LΔF**/**fMLF** (1:0.25), different drugs at a concentration of 4 mM were individually entrapped. The drugs isoniazid, amphotericin B, and ciprofloxacin were chosen for the following reasons. Isoniazid and amphotericin B are standard drugs used for killing the macrophage intracellular pathogen *Mycobacterium tuberculosis*, a causative agent of tuberculosis, and *Leishmania donovani*, a causative agent of leishmaniasis. Ciprofloxacin is a standard antibiotic used to treat wound infections, and it is effective against numerous devastating bacterial species including *Klebsiella pneumoniae*, methicillin-susceptible *Staphylococcus aureus*, and *Streptococcus pyogenes*.

The percentage of drug release from the nanofiber gel matrix into the overlaying phosphate-buffered saline at pH 7.4 was quantified by means of UV/Vis spectroscopy. Figure 1H shows the release profiles of these three drugs from the hydrogel over a span of 5 days. As seen from the drug release profiles, the coassembled hydrogels exhibit a slow and continuous release of the entrapped drugs as opposed to a burst release. The dissimilarity of the release profiles can be attributed to the different net charge, molecular weight, and hydrophobicity of the molecules (Figure S10). All three have no net charge at neutral pH and so their charge-based interactions with the hydrogel network can be ruled out. Release is slowed as molecular weight and hydrophobicity increase.

To achieve controlled and effective drug delivery, fine-tuning the factors that can increase or decrease the amount of drug released from the hydrogel matrix over time is essential. One such regulatory factor is the mesh size of the hydrogel, which is a concentration-dependent property. **LΔF** has been reported to show self-assembly into nanogels or hydrogels in a concentration-dependent manner.[9] Nanogels are a nanoparticulate form of hydrogels. At 0.3−0.4% w/v it exists as a nanogel, while at concentrations higher than 0.5% w/v it forms self-supporting hydrogels. At 0.3% w/v, it exhibits a network of small fibers of length 100 nm with higher mesh size, while at 0.4% w/v it shows relatively longer fibers with a decreased mesh size. Within the hydrogel regime, the mesh size decreases further with an increase in peptide concentration. For this reason, we investigated the influence of **LΔF**/**fMLF** (1:0.25) coassembly concentration on ciprofloxacin release. To this end 4 mM ciprofloxacin was entrapped in 0.5, 1, or 2% w/v hydrogels, and its release profile determined as above. Figure 1I shows that the hydrogelator concentration does affect the drug release, as the percentage drug released from the 2% w/v hydrogel is about 50% lower than in the case of 0.5% w/v after 120 h. The coassembled gels 1% w/v **LΔF** + **fMLF** (1:0.25) also showed ability to entrap and release interleukin-4 in a slow and continuous manner for a duration of about 6 days (Figure S11).

CONCLUSIONS

In summary, a coassembly strategy to generate multivalent supramolecular peptide hydrogel scaffolds that can act as wound dressing materials was investigated. The dipeptide hydrogelator **LΔF** and the macrophage chemotactic peptide ligand **fMLF** were coassembled and the properties of the resulting hydrogels were determined by a variety of means. CD spectroscopy demonstrated that coassembly did not change the secondary structural features of **LΔF**, whereas rheology indicated that the mechanical strength and injectability of the gels remains unaltered. Electron micrographs suggest an increase in nanofiber thickness with increasing ligand density, whereas EDX analysis shows that the coassembled nanofibers are composed of both peptides based on the presence of a sulfur signal. The **fMLF** ligand in the coassembled gel was found to attract macrophage. As macrophage recruitment is important in wound healing, wherein it activates several other cascades of events by producing GFs; this property is highly advantageous. The hydrogel matrix has the ability to entrap and release different types of drugs in a slow and continuous manner. One of the drugs investigated here is ciprofloxacin, an antibiotic that can prevent wound site infections. The impact of mesh size on drug release was also investigated. The ability of these coassembled hydrogels to support three-dimensional growth of macrophages and fibroblasts was demonstrated by means of confocal microscopy. All these features indicate the potential of this coassembled hydrogel to be developed as a wound-dressing material in treating chronic conditions like DFU. The kind of simple molecular coassembly approach to identifying bioactive ultrashort peptide hydrogelators shown here can be used for a significant expansion of the repertoire of such functional biomaterials for nanomedicine-based applications.

EXPERIMENTAL SECTION

Cryo-TEM Sample Preparation and Analysis. Droplets (5 μL) of aqueous samples of **LΔF** and **LΔF**/**fMLF** at molar ratios of 1:0.25, 1:0.5, and 1:1 in 0.8 M sodium acetate buffer at pH 7.4 were placed on hydrophilized [plasma treatment using a BALTEC MED 020 device (Leica Microsystems, Wetzlar, Germany)], perforated carbon filmed grids (Quantifoil Micro Tools GmbH, Jena, Germany). Excess fluid was blotted off to create an ultrathin layer (typical thickness 200−300 nm) of the solution, which spanned the holes of the support film. The prepared samples were immediately vitrified by propelling the grids into liquid ethane at its freezing point (−184 °C). The vitrified sample grids were transferred under liquid nitrogen by the use of a Gatan (Pleasanton, CA, USA) cryo-holder (model 626) into a Tecnai F20 TEM (FEI company, Oregon, USA) equipped with FEG and operated at 160 kV acceleration voltage. Microscopy was carried out at −175 °C sample temperature using the microscope's low dose protocol at calibrated primary magnifications of 50k or 29k. The defocus was set to be 3.98 or 9.81 μm, respectively. Images were recorded by the use of a 4k-Eagle CCD camera (FEI Company, Oregon, USA) at 2k resolution (binning 2).

https://dx.doi.org/10.1021/acsomega.9b04371
ACS Omega 2020, 5, 8557−8563

3D Cell Viability and Growth. 1% w/v **LΔF/fMLF** (1:0.25) hydrogels were prepared in 8-well plates and incubated in a cell culture hood overnight to allow methanol evaporation. Subsequently, 200 μL of Dulbecco's modified Eagle's medium (DMEM) with a density of 1×10^4 fibroblast cells per well were transferred onto the gel surface and incubated with 5% CO_2 at 37 °C overnight. Nonadherent cells were aspirated, and the plates were maintained in the incubator for 15 days with continuous exchange of spent media with fresh DMEM. The cells that adhered and migrated into the gels were stained with Calcein-AM and observed under confocal microscopy. Untreated cells served as the control. For the 3D growth of U937 cells 1% w/v **LΔF/fMLF** (1:0.25), hydrogels were prepared in 8-well plates and left in a cell culture hood overnight to allow methanol evaporation. Subsequently, 200 μL RPMI with a density of 1.5×10^6 U937 cells per mL were transferred onto the gel surface and incubated with 5% CO_2 at 37 °C for 24 h. Nonadherent cells were aspirated, and adherent cells differentiated into macrophages by treating the gels with RPMI containing 100 nM phorbol 12-myristate 13-acetate (Sigma Aldrich) for a duration of 24 h, followed by incubation in RPMI media for another 24 h. The cells were further differentiated to M2 polarization by treating the gels with IL-4 (20 ng per mL) for the next 72 h. Subsequent cultivation was done in RPMI media for the next 9 days with continuous exchange of spent media with fresh media. The cells that adhered and migrated into the gels were stained with LIVE/DEAD Viability/Cytotoxicity Kit (Invitrogen) and observed under confocal microscopy. Untreated cells served as the control. To quantify growth, fibroblasts were cultured in 1% w/v **LΔF/fMLF** (1:0.25) hydrogels under conditions described above. At predetermined time intervals from day 0 to day 14, the cell culture media in the plates was replaced with 10% (v/v) PrestoBlue-fresh medium mixture for 3 h. After incubation, 100 μL of this media is removed and its fluorescence intensity is monitored at excitation 550 nm and emission 590 nm. Analysis was done in triplicate (Figure S9).

Chemotactic Assay. A chemotactic assay was conducted for 1% w/v **LΔF/fMLF** (1: 0.25) hydrogels by means of CytoSelectTM 24-well cell migration assay kit (Cell biolabs, INC) containing 5 μm pore size PET membrane inserts in a 24-well plate. The migratory cells were quantified by CyQuant GR Dye (Invitrogen). A well containing only **LΔF** gel and another containing only cell culture media (without any gel) served as negative controls, while soluble **fMLF** peptide at an equimolar concentration served as a positive control. The test samples were normalized to the fluorescence of **fMLF** exposed samples and were multiplied by 100%.

■ ASSOCIATED CONTENT

Supporting Information

The Supporting Information is available free of charge at https://pubs.acs.org/doi/10.1021/acsomega.9b04371.

Experimental details for sample synthesis/purification/coassembly; EDX data; cryo-TEM data and images; SEM images; CD spectra; cytotoxicity data; proliferation data; and drug data (PDF)

■ AUTHOR INFORMATION

Corresponding Author

Beate Koksch − *Department of Chemistry and Biochemistry, Freie Universität Berlin, 14195 Berlin, Germany;* orcid.org/0000-0002-9747-0740; Phone: +49-30-838-55344; Email: beate.koksch@fu-berlin.de

Authors

Chaitanya Kumar Thota − *Department of Chemistry and Biochemistry, Freie Universität Berlin, 14195 Berlin, Germany*

Allison A. Berger − *Department of Chemistry and Biochemistry, Freie Universität Berlin, 14195 Berlin, Germany*

Laura Elomaa − *Department of Chemistry and Biochemistry, Freie Universität Berlin, 14195 Berlin, Germany*

Chaunxiong Nie − *Department of Chemistry and Biochemistry, Freie Universität Berlin, 14195 Berlin, Germany*

Christoph Böttcher − *Research Center for Electron Microscopy, Freie Universität Berlin, 14195 Berlin, Germany*

Complete contact information is available at: https://pubs.acs.org/10.1021/acsomega.9b04371

Author Contributions

C.T. and B.K. designed the experiments; C.T. synthesized compounds; characterization was conducted by C.T. and C.B.; biological activity determination was carried out by C.T., L. E., and C. X.; data were analyzed by C.T. and B.K. The manuscript was written through contributions of all authors. All authors have given approval to the final version of the manuscript.

Funding

We thank the Collaborative Research Center 765 (SFB765/2-2014) of the Deutsche Forschungsgemeinschaft (DFG) for the generous financial support.

Notes

The authors declare no competing financial interest.

■ ACKNOWLEDGMENTS

We would like to acknowledge the assistance of the Core Facility BioSupraMol supported by the DFG.

■ ABBREVIATIONS

DFU; diabetic foot ulcer; Δ*F*; *α,β*-dehydrophenylalanine; TEM; transmission electron microscopy; SEM; scanning electron microscopy; CD; circular dichroism spectroscopy; EDX; energy-dispersive X-ray spectroscopy; HEK293T; human embryonic kidney 293 cells; CCK8; cell counting kit 8

■ REFERENCES

(1) Li, J.; Xing, R.; Bai, S.; Yan, X. Recent Advances of Self-Assembling Peptide-Based Hydrogels for Biomedical Applications. *Soft Matter* **2019**, *15*, 1704−1715.

(2) Wakabayashi, R.; Suehiro, A.; Goto, M.; Kamiya, N. Designer Aromatic Peptide Amphiphiles for Self-Assembly and Enzymatic Display of Proteins with Morphology Control. *Chem. Commun.* **2019**, *55*, 640−643.

(3) Kulkarni, K.; Habila, N.; Del Borgo, M. P.; Aguilar, M.-I. Novel Materials From the Supramolecular Self-Assembly of Short Helical B3-Peptide Foldamers. *Front. Chem.* **2019**, *7*, 1−12.

(4) Dasgupta, A.; Mondal, J. H.; Das, D. Peptide Hydrogels. *RSC Adv.* **2013**, *3*, 9117−9149.

(5) Hauser, C. A. E.; Zhang, S. Designer Self-Assembling Peptide Nanofiber Biological Materials. *Chem. Soc. Rev.* **2010**, *39*, 2780−2790.

(6) Adler-Abramovich, L.; Gazit, E. The Physical Properties of Supramolecular Peptide Assemblies: From Building Block Association to Technological Applications. *Chem. Soc. Rev.* **2014**, *43*, 6881−6893.

(7) Lee, J.; Choe, I. R.; Kim, N.-K.; Kim, W.-J.; Jang, H.-S.; Lee, Y.-S.; Nam, K. T. Water-Floating Giant Nanosheets from Helical Peptide Pentamers. *ACS Nano* **2016**, *10*, 8263−8270.

(8) Jang, H.-S.; Lee, J.-H.; Park, Y.-S.; Kim, Y.-O.; Park, J.; Yang, T.-Y.; Jin, K.; Lee, J.; Park, S.; You, J. M.; et al. Tyrosine-Mediated Two-Dimensional Peptide Assembly and Its Role as a Bio-Inspired Catalytic Scaffold. *Nat. Commun.* **2014**, *5*, 3665.
(9) Thota, C. K.; Yadav, N.; Chauhan, V. S. A Novel Highly Stable and Injectable Hydrogel Based on a Conformationally Restricted Ultrashort Peptide. *Sci. Rep.* **2016**, *6*, 31167.
(10) Fichman, G.; Gazit, E. Self-Assembly of Short Peptides to Form Hydrogels: Design of Building Blocks, Physical Properties and Technological Applications. *Acta Biomater.* **2014**, *10*, 1671−1682.
(11) Draper, E. R.; Morris, K. L.; Little, M. A.; Raeburn, J.; Colquhoun, C.; Cross, E. R.; McDonald, T. O.; Serpell, L. C.; Adams, D. J. Hydrogels Formed from Fmoc Amino Acids. *CrystEngComm* **2015**, *17*, 8047−8057.
(12) Adler-Abramovich, L.; Vaks, L.; Carny, O.; Trudler, D.; Magno, A.; Caflisch, A.; Frenkel, D.; Gazit, E. Phenylalanine Assembly into Toxic Fibrils Suggests Amyloid Etiology in Phenylketonuria. *Nat. Chem. Biol.* **2012**, *8*, 701.
(13) Fichman, G.; Guterman, T.; Adler-Abramovich, L.; Gazit, E. Synergetic Functional Properties of Two-Component Single Amino Acid-Based Hydrogels. *CrystEngComm* **2015**, *17*, 8105−8112.
(14) Orbach, R.; Adler-Abramovich, L.; Zigerson, S.; Mironi-Harpaz, I.; Seliktar, D.; Gazit, E. Self-Assembled Fmoc-Peptides as a Platform for the Formation of Nanostructures and Hydrogels. *Biomacromolecules* **2009**, *10*, 2646−2651.
(15) Ryan, D. M.; Anderson, S. B.; Nilsson, B. L. The Influence of Side-Chain Halogenation on the Self-Assembly and Hydrogelation of Fmoc-Phenylalanine Derivatives. *Soft Matter* **2010**, *6*, 3220−3231.
(16) Woolfson, D. N.; Mahmoud, Z. N. More than Just Bare Scaffolds: Towards Multi-Component and Decorated Fibrous Biomaterials. *Chem. Soc. Rev.* **2010**, *39*, 3464−3479.
(17) Liu, R.; Hudalla, G. A. Using Self-Assembling Peptides to Integrate Biomolecules into Functional Supramolecular Biomaterials. *Molecules* **2019**, *24*, 1450.
(18) Guttenplan, A. P. M.; Young, L. J.; Matak-Vinkovic, D.; Kaminski, C. F.; Knowles, T. P. J.; Itzhaki, L. S. Nanoscale Click-Reactive Scaffolds from Peptide Self-Assembly. *J. Nanobiotechnol.* **2017**, *15*, 70.
(19) Fan, Q.; Yujie, J.; Jingjing, W.; Li, W.; Weidong, L.; Rui, C.; Zhipeng, C. Self-Assembly Behaviours of Peptide−Drug Conjugates: Influence of Multiple Factors on Aggregate Morphology and Potential Self-Assembly Mechanism. *R. Soc. Open Sci.* **2018**, *5*, 172040.
(20) Cheng, B.; Yan, Y.; Qi, J.; Deng, L.; Shao, Z.-W.; Zhang, K.-Q.; Li, B.; Sun, Z.; Li, X. Cooperative Assembly of a Peptide Gelator and Silk Fibroin Afford an Injectable Hydrogel for Tissue Engineering. *ACS Appl. Mater. Interfaces* **2018**, *10*, 12474−12484.
(21) Halperin-Sternfeld, M.; Adler-Abramovich, L.; Sevostianov, R.; Grigoriants, I.; Ghosh, M. Molecular Co-Assembly as a Strategy for Synergistic Improvement of the Mechanical Properties of Hydrogels. *Chem. Commun.* **2017**, *53*, 9586−9589.
(22) Makam, P.; Gazit, E. Minimalistic Peptide Supramolecular Co-Assembly: Expanding the Conformational Space for Nanotechnology. *Chem. Soc. Rev.* **2018**, *47*, 3406−3420.
(23) Nagy-Smith, K.; Beltramo, P. J.; Moore, E.; Tycko, R.; Furst, E. M.; Schneider, J. P. Molecular, Local, and Network-Level Basis for the Enhanced Stiffness of Hydrogel Networks Formed from Coassembled Racemic Peptides: Predictions from Pauling and Corey. *ACS Cent. Sci.* **2017**, *3*, 586−597.
(24) Wan, L.; Zhang, X.; Pooyan, S.; Palombo, M. S.; Leibowitz, M. J.; Stein, S.; Sinko, P. J. Optimizing Size and Copy Number for PEG-FMLF (N-Formyl-Methionyl-Leucyl-Phenylalanine) Nanocarrier Uptake by Macrophages. *Bioconjugate Chem.* **2008**, *19*, 28−38.
(25) Pooyan, S.; Qiu, B.; Chan, M. M.; Fong, D.; Sinko, P. J.; Leibowitz, M. J.; Stein, S. Conjugates Bearing Multiple Formyl-Methionyl Peptides Display Enhanced Binding to but Not Activation of Phagocytic Cells. *Bioconjugate Chem.* **2002**, *13*, 216−223.
(26) Wan, L.; Pooyan, S.; Hu, P.; Leibowitz, M. J.; Stein, S.; Sinko, P. J. Peritoneal Macrophage Uptake, Pharmacokinetics and Biodistribution of Macrophage-Targeted PEG-FMLF (N-Formyl-Methionyl-Leucyl-Phenylalanine) Nanocarriers for Improving HIV Drug Delivery. *Pharm. Res.* **2007**, *24*, 2110−2119.
(27) Feng, Y.; Li, Q.; Wu, D.; Niu, Y.; Yang, C.; Dong, L.; Wang, C. Biomaterials A Macrophage-Activating , Injectable Hydrogel to Sequester Endogenous Growth Factors for in Situ Angiogenesis. *Biomaterials* **2017**, *134*, 128−142.
(28) Sun, G.; Reinblatt, M.; Dickinson, L. E.; Fox-Talbot, K.; Zhang, X.; Sebastian, R.; Shen, Y.-I.; Harmon, J. W.; Steenbergen, C.; Gerecht, S. Dextran Hydrogel Scaffolds Enhance Angiogenic Responses and Promote Complete Skin Regeneration during Burn Wound Healing. *Proc. Natl. Acad. Sci. U. S. A.* **2011**, *108*, 20976−20981.
(29) Liu, H.; Wang, C.; Li, C.; Qin, Y.; Wang, Z.; Yang, F.; Li, Z.; Wang, J. A Functional Chitosan-Based Hydrogel as a Wound Dressing and Drug Delivery System in the Treatment of Wound Healing. *RSC Adv.* **2018**, *8*, 7533−7549.
(30) Mitragotri, S.; Burke, P. A.; Langer, R. Overcoming the Challenges in Administering Biopharmaceuticals: Formulation and Delivery Strategies. *Nat. Rev. Drug Discovery* **2014**, *13*, 655.
(31) Amsden, B. Novel Biodegradable Polymers for Local Growth Factor Delivery. *Eur. J. Pharm. Biopharm.* **2015**, *97*, 318−328.
(32) Simons, M.; Bonow, R. O.; Chronos, N. A.; Cohen, D. J.; Giordano, F. J.; Hammond, H. K.; Laham, R. J.; Li, W.; Pike, M.; Sellke, F. W.; et al. Clinical Trials in Coronary Angiogenesis: Issues, Problems, Consensus. *Circulation* **2000**, *102*, e73−e86.
(33) Carrejo, N. C.; Moore, A. N.; Silva, T. L. L.; Leach, D. G.; Li, I.; Walker, D. R.; Hartgerink, D. Multidomain Peptide Hydrogel Accelerates Healing of Full-Thickness Wounds in Diabetic Mice. *ACS Biomaterials Science & Engineering* **2018**, *4*, 1386.
(34) Lokhande, G.; Carrow, J. K.; Thakur, T.; Xavier, J. R.; Parani, M.; Bayless, K. J.; Gaharwar, A. K. Nanoengineered Injectable Hydrogels for Wound Healing Application. *Acta Biomater.* **2018**, *70*, 35−47.
(35) Chen, H.; Cheng, R.; Zhao, X.; Zhang, Y.; Tam, A.; Yan, Y.; Shen, H.; Zhang, Y. S.; Qi, J.; Feng, Y.; et al. An Injectable Self-Healing Coordinative Hydrogel with Antibacterial and Angiogenic Properties for Diabetic Skin Wound Repair. *NPG Asia Mater.* **2019**, *11*, 3.
(36) Schneider, J. P.; Pochan, D. J.; Ozbas, B.; Rajagopal, K.; Pakstis, L.; Kretsinger, J. Responsive Hydrogels from the Intramolecular Folding and Self-Assembly of a Designed Peptide. *J. Am. Chem. Soc.* **2002**, *124*, 15030−15037.
(37) Yan, C.; Altunbas, A.; Yucel, T.; Nagarkar, R. P.; Schneider, J. P.; Pochan, D. J. Injectable Solid Hydrogel: Mechanism of Shear-Thinning and Immediate Recovery of Injectable β-Hairpin Peptide Hydrogels. *Soft Matter* **2010**, *6*, 5143−5156.
(38) Wang, H.; Luo, Z.; Wang, Y.; He, T.; Yang, C.; Ren, C.; Ma, L.; Gong, C.; Li, X.; Yang, Z. Enzyme-Catalyzed Formation of Supramolecular Hydrogels as Promising Vaccine Adjuvants. *Adv. Funct. Mater.* **2016**, *26*, 1822−1829.
(39) Vilaça, H.; Castro, T.; Costa, F. M. G.; Melle-Franco, M.; Hilliou, L.; Hamley, I. W.; Castanheira, E. M. S.; Martins, J. A.; Ferreira, P. M. T. Self-Assembled RGD Dehydropeptide Hydrogels for Drug Delivery Applications. *J. Mater. Chem. B* **2017**, *5*, 8607−8617.
(40) Nandi, N.; Gayen, K.; Ghosh, S.; Bhunia, D.; Kirkham, S.; Sen, S. K.; Ghosh, S.; Hamley, I. W.; Banerjee, A. Amphiphilic Peptide-Based Supramolecular, Noncytotoxic, Stimuli-Responsive Hydrogels with Antibacterial Activity. *Biomacromolecules* **2017**, *18*, 3621−3629.
(41) Chen, S.; Zhang, M.; Shao, X.; Wang, X.; Zhang, L.; Xu, P.; Zhong, W.; Zhang, L.; Xing, M.; Zhang, L. A Laminin Mimetic Peptide SIKVAV-Conjugated Chitosan Hydrogel Promoting Wound Healing by Enhancing Angiogenesis, Re-Epithelialization and Collagen Deposition. *J. Mater. Chem. B* **2015**, *3*, 6798−6804.
(42) Majumder, P.; Baxa, U.; Walsh, S. T. R.; Schneider, J. P. Design of a Multicompartment Hydrogel That Facilitates Time-Resolved Delivery of Combination Therapy and Synergized Killing of Glioblastoma. *Angew. Chem., Int. Ed.* **2018**, *57*, 15040−15044.

https://dx.doi.org/10.1021/acsomega.9b04371
ACS Omega 2020, 5, 8557−8563

(43) Miller, S. E.; Yamada, Y.; Patel, N.; Suárez, E.; Andrews, C.; Tau, S.; Luke, B. T.; Cachau, R. E.; Schneider, J. P. Electrostatically Driven Guanidinium Interaction Domains That Control Hydrogel-Mediated Protein Delivery In Vivo. *ACS Cent. Sci.* **2019**, *5*, 1750−1759.
(44) Lindsey, S.; Piatt, J. H.; Worthington, P.; Sönmez, C.; Satheye, S.; Schneider, J. P.; Pochan, D. J.; Langhans, S. A. Beta Hairpin Peptide Hydrogels as an Injectable Solid Vehicle for Neurotrophic Growth Factor Delivery. *Biomacromolecules* **2015**, *16*, 2672−2683.
(45) Naskar, J.; Palui, G.; Banerjee, A. Tetrapeptide-Based Hydrogels: For Encapsulation and Slow Release of an Anticancer Drug at Physiological PH. *J. Phys. Chem. B* **2009**, *113*, 11787−11792.
(46) Baral, A.; Roy, S.; Dehsorkhi, A.; Hamley, I. W.; Mohapatra, S.; Ghosh, S.; Banerjee, A. Assembly of an Injectable Noncytotoxic Peptide-Based Hydrogelator for Sustained Release of Drugs. *Langmuir* **2014**, *30*, 929−936.

https://dx.doi.org/10.1021/acsomega.9b04371
ACS Omega 2020, 5, 8557−8563